

# Spontaneous Solution-Phase Redox Deposition of a Dense Cobalt(II) Phthalocyanine Monolayer on Gold

Ursula Mazur, Maya Leonetti, William A. English, and K. W. Hipps\*

*Department of Chemistry and Materials Science Program, Washington State University, Pullman, Washington 99164-4630*

*Received: May 25, 2004; In Final Form: June 4, 2004*

A dense monolayer of cobalt(II) phthalocyanine, CoPc, can be formed on a gold surface by spontaneous redox deposition followed by vacuum annealing at about 110 °C. CsCoPc(CN)<sub>2</sub> or KCoPc(CN)<sub>2</sub> in dilute (~10<sup>-6</sup> M) ethanol solution rapidly forms a dense adlayer that, when washed with ethanol, can be imaged by scanning tunneling microscopy, STM, in air. This adlayer is converted to a monolayer of CoPc by vacuum annealing as confirmed by STM and X-ray photoelectron spectroscopy (XPS). This spontaneous surface redox adsorption process represents a novel method for depositing metallorganic complexes, which are ultimately only physisorbed on gold.

## Introduction

Phthalocyanine (Pc) and porphyrin-based (P) electrical conductors are used extensively as building blocks for constructing stable 2D supermolecular electronic assemblies. The architectural forms of these structures include simple clusters, wires, arrays, and even designer surfaces.<sup>1-7</sup> Understanding the principles of architecture and the ability to control Pc assembly on surfaces continues to be of critical importance in the rational design and construction of functional optoelectronic nanoscale devices derived from phthalocyanines and porphyrins. The most basic monolayer architectures arise from vapor deposition. Simple complexes deposited on conductive surfaces in vacuum or from solution exhibit a close-packed arrangement that results from van der Waal's interactions between the molecules.<sup>2-4</sup> Hipps and co-workers vapor deposited different 2D metal phthalocyanine and porphyrin assemblies on gold and imaged them by UHV scanning tunneling microscopy (STM) with remarkable submolecular resolution.<sup>2,3,6</sup> Bai demonstrated that monolayer molecular arrays of alkane-derivitized phthalocyanine can be assembled from solution on straight-chain alkane templates deposited on graphite.<sup>4</sup> Recently, Itaya formed both a pure MPc and a mixed CoPc and copper tetraphenylporphyrin (CuTPP) adlayer by immersing a Au single crystal into a benzene solution containing the parent compounds. By imaging the adsorbate system in aqueous solution, he demonstrated a structural dependence of the adlayer on the crystallographic orientation of the gold surface.<sup>5</sup>

The 2D self-assembly of adsorbed Pc and P molecules also can be directed by selectively controlling noncovalent intermolecular interactions such as van der Waals attraction and hydrogen bonding.<sup>6-8</sup> The best-known examples of hydrogen bonding-driven surface assembly include data reported by Hipps, Yokoyama, and Griessl. Hipps and co-workers found the formation of a new well-ordered 2D structure with 1:1 stoichiometry of F<sub>16</sub>CoPc and NiTPP on gold by vapor-phase deposition in UHV.<sup>6</sup> Yokoyama observed small clusters and chains of CN-substituted porphyrins vacuum deposited on Au(111) in a low-temperature STM environment.<sup>7</sup> Griessl and co-workers

studied the extensive hydrogen bonding networks formed by trimesic acid on graphite.<sup>8</sup>

All of the above methods for monolayer formation share a common failing—they produce monolayers that are not substrate location-selective. Because the final layer is physisorbed rather than chemisorbed, almost any surface the adsorbate hits will support it (snow on a field). Given a complex device structure with exposed surfaces of various metals and semiconductors, all of the surfaces will be coated.

A pathway to the 2D architecture of physisorbed complex molecules that has not been explored is the formation of self-organized molecular monolayers by spontaneous redox processes at the substrate surface. In this report, we present a generalized approach where a soluble species having a redox reaction induced by a metal electrode spontaneously decomposes to a well ordered physisorbed layer of insoluble product upon electrical contact with that metal. The chemistry described here is very different from that of the conventional thiol or thiolate precursor SAM films. In those systems, the final monolayer is chemisorbed to the substrate surface.<sup>9</sup> The procedure presented here does not require complex vacuum technology. Rather, it relies on solubility partitioning between solution and adsorbed phases, and it can create very reproducible well-ordered submonolayers, monolayers, and multilayers. We note that we previously observed the conversion of soluble FePcCl to insoluble FePc by spontaneous reduction on an aluminum surface.<sup>10</sup> In that work, however, we did not determine the surface structure of the adsorbed layer.

Here we demonstrate the formation a stable 2D assembly of CoPc from solution via spontaneous redox reactions between a biaxially substituted dicyano cobalt phthalocyanine salt, MCoPc(CN)<sub>2</sub> (M = K, Cs), and a gold substrate. We selected the CoPc(CN)<sub>2</sub><sup>-1</sup> ion (shown in Figure 1) because of its chemical stability and solubility in simple organic solvents. Its X-ray structure has been reported.<sup>11</sup>

The process by which the CoPc adlayer is formed on the gold electrode can be elucidated in part from the cyclic voltammetry (CV) studies of MCoPc(CN)<sub>2</sub> reported by Hanack and co-workers.<sup>12</sup> On the basis of their voltammetric data, Hanack proposed that in acetone MCoPc(CN)<sub>2</sub> is oxidized to a

\* Corresponding author. E-mail: hipps@wsu.edu.

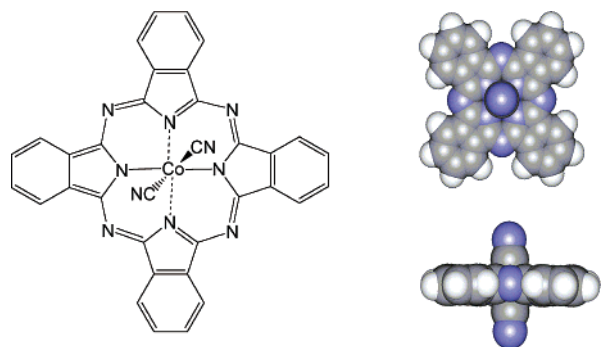


**Figure 1.** Molecular structure of the  $\text{CoPc}(\text{CN})_2^-$  ion, which measures approximately 1.4 nm across and 0.61 nm along the NC–Co–CN fragment.

92 neutral radical,  $\text{CoPc}(\text{CN})_2$ . The oxidation potential ( $E_{1/2}$ ) of  
 93  $\text{MCoPc}(\text{CN})_2$  in acetone and 0.1 M  $\text{Bu}_4\text{NClO}_4$  was measured  
 94 at 0.88 V (sce). Applying our orbital-mediated tunneling (OMT)  
 95 model to this process, we predict that an  $E_{1/2(\text{oxd})}$  of 0.88 V (sce)  
 96 is equivalent to 5.29 V relative to the vacuum state.<sup>10</sup> That value  
 97 is very close to the measured work function for Au(111), 5.3  
 98 V. Thus, we expect  $\text{CoPc}(\text{CN})_2^-$  in contact with the Au(111)  
 99 to oxidize spontaneously to the radical. We have found that the  
 100  $\text{CoPc}(\text{CN})_2$  radical then follows a complex redox pathway with  
 101 the eventual formation of neutral and insoluble CoPc derivative  
 102 species adsorbed on the gold surface. Upon low temperature  
 103 (110 °C) annealing in vacuum, this monolayer converts completely  
 104 to cobalt(II) phthalocyanine. We note here that the isolated  
 105  $\text{MCoPc}(\text{CN})_2$  salt is stable to 300 °C before the first  
 106 cyanide is cleaved from the cobalt ion.<sup>13</sup>

## 107 Experimental Section

108 The ionic complex,  $\text{MCoPc}(\text{CN})_2$  ( $M = \text{K}$  or  $\text{Cs}$ ), was  
 109 prepared and purified by published methods.<sup>13</sup> Elemental  
 110 analysis, <sup>1</sup>H NMR, and infrared spectroscopy confirmed the  
 111 purity. Well-organized phthalocyanine monolayers on Au(111)  
 112 were formed by exposing freshly annealed Au(111) substrates  
 113 to a  $10^{-6}$  M ethanolic solution of the  $\text{MCoPc}(\text{CN})_2$  complex  
 114 for 10 min, washing with a small amount of ethanol, and drying  
 115 under a gentle flow of inert gas for 15 min. A high-vacuum  
 116 multipurpose deposition chamber was used for the preparation  
 117 of CoPc submonolayers on Au(111)/mica samples by vapor  
 118 deposition. CoPc was purchased from Strem Chemicals<sup>14</sup> and  
 119 twice sublimed before it was deposited from a tantalum box  
 120 source. Both solution- and vacuum-deposited samples were  
 121 transported in air to the load lock of the XPS where they were  
 122 analyzed under UHV.

123 Scanning tunneling microscopy (STM) was performed both  
 124 in air and in UHV. The ambient STM images were collected  
 125 using a Digital Instruments stand alone head and a Nanoscope  
 126 E controller, and the UHV STM data were obtained with an  
 127 RHK Technology<sup>15</sup> microscope (model UHV300) and control  
 128 electronics (model SPM100). Images were plane fit and low-  
 129 pass filtered. STM tips were prepared from 0.25-mm W by  
 130 electrochemical etching or from  $\text{Pt}_{0.8}\text{Ir}_{0.2}$  wire by mechanical  
 131 cutting. W tips always required additional cleaning once in  
 132 UHV. XPS analysis was performed on a Kratos Axis-165  
 133 electron spectrometer having a base pressure of  $5 \times 10^{-10}$  Torr.  
 134 Monochromatic radiation from an Al  $K\alpha$  X-ray source was used  
 135 for excitation. Samples could be heated and cooled in place in  
 136 the XPS system.

## 137 Results and Discussion

138 Solution-grown specimens were first examined in air by STM  
 139 and then transferred into the UHV chamber housing either the  
 140 RHK STM or the XPS system. Parts a and b of Figure 2 show  
 141 typical large-scale STM images of Pc adlayers formed by  
 142 exposing Au(111) to  $\text{KCoPc}(\text{CN})_2$  solution. Samples were  
 143 washed with ethanol and dried prior to measurement. Similar  
 144 results were obtained from  $\text{CsCoPc}(\text{CN})_2$  solution. Image 2a  
 145 was acquired in air. Micrographs such as 2a were obtained with  
 146 a high level of reproducibility, and samples were stable for at  
 147 least 1 day when stored in a desiccator. Images b and c of Figure  
 148 2 were obtained in an UHV environment after annealing the  
 149 solution-grown sample at 110 °C for a few minutes.

150 Large-scale images show well-ordered 2D assemblies with  
 151 distinct molecules. Measurements made in air also show random  
 152 groupings of molecules well separated from islands and high  
 153 spots associated either with axially substituted phthalocyanines  
 154 or adsorbates on the Pc layer. These isolated molecules and  
 155 small clusters are not usually observed at room temperature in  
 156 CoPc films vapor deposited on Au because the CoPc–Au  
 157 interaction is too weak and there is rapid diffusion of molecules  
 158 between islands. We were unable to obtain submolecular  
 159 resolution images in air. This may be due to the mixed  
 160 composition of the initially formed layer (vide infra) or to a  
 161  $\text{CoPc}-\text{O}_2$  adduct that may form under these conditions.<sup>16</sup>

162 It is useful to note that the STM image obtained in air from  
 163 the as-deposited solution is less densely packed than that of  
 164 the annealed monolayer. Figure 2a shows rows with an internal  
 165 spacing of about 1.2 nm but a row–row spacing of about 1.7  
 166 nm. In contrast, the interatomic spacing in parts b and c of Figure  
 167 2 is 1.2 nm in any direction. After annealing, the structure is  
 168 defined by a much denser square unit cell. The origin of this  
 169 structural change is still unclear but is probably related to the

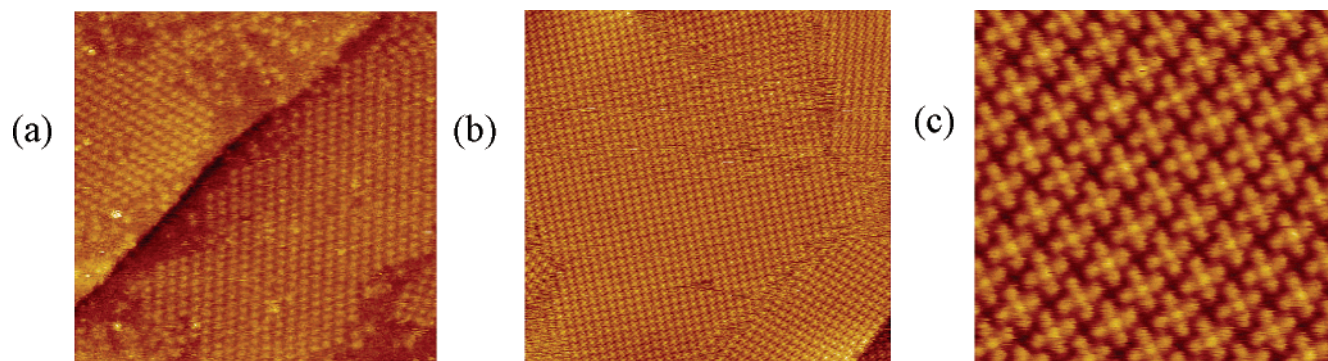


**Figure 2.** STM micrographs of Au(111) exposed to  $10^{-6}$  M ethanolic  $\text{KCoPc}(\text{CN})_2$  for 10 min and washed with ethanol: (a)  $50 \times 50 \text{ nm}^2$  image acquired in air with 0.8-V bias voltage and 180-pA tunneling current, (b)  $50 \times 50 \text{ nm}^2$  image, and (c) high-resolution  $10 \times 10 \text{ nm}^2$  image. Both b and c were obtained under UHV conditions after annealing at 110 °C. Sample bias and tunneling current were +0.32 and +0.75 V and 100 pA, respectively, for images b and c. A PtIr tip was used for all three images.

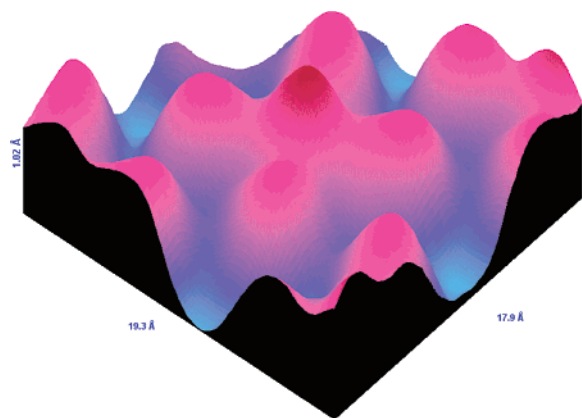


**Figure 3.** Correlation-averaged 3D image of a single CoPc molecule on Au formed from redox adsorption from solution.

mixed composition (vide infra) of the as-formed monolayer. Alternatively, the coadsorption of solvent may also influence the as-grown structure.

Details of the internal structure, orientation, and packing of the adsorbed complex are seen in the high-resolution image (Figure 2c) obtained in UHV after sample annealing. Individual phthalocyanine molecules can be recognized by their clover-leaf shapes with a central peak and four additional spots at the corners. To better define the single-molecule constant current contour, we performed a correlation average on the data in Figure 2c, and a highly accurate image results (Figure 3). In this low-noise, high-resolution image, one may observe that the benzene rings of the Pc ring are more effective conductors than the five-membered rings. The large characteristic increase in the tunneling probability at the center of the molecule has been attributed to the half-filled  $d_{z^2}$  orbital acting as an atomic wire. The apparent height at the molecular center is lower than expected for the case of cyano substitution, but this is NOT a definitive test. Note that although alkali ions can be observed in STM<sup>17</sup> no features attributable to either potassium or cesium ions have been seen in our STM studies.

XPS analysis of both the unannealed and annealed CsCoPc-(CN)<sub>2</sub> ethanolic solution samples (after washing) shows that there is less than 5% of the expected Cs/Co ratio. That is, there was no detectable Cs in the XPS of the adsorbed film. Thus, the surface species is clearly a neutral complex. The Co 2p region of the XPS is also very informative. Initially (lower curve of Figure 4) there are both Co<sup>2+</sup> and Co<sup>3+</sup> species present on the surface, with peaks near 778.2 and 780.2 eV assigned to the 2p<sub>3/2</sub> transition in Co<sup>2+</sup> and those near 779.7 and 781.1 eV being due to Co<sup>3+</sup>. With annealing at 100 °C for 10 min, most of the surface layer has been converted to Co<sup>2+</sup>. After annealing at 110 °C, the Co 2p XPS becomes identical to that of authentic CoPc (top curve of Figure 4).

Our interpretation of these results is that the initial monolayer is a mixture of CoPc and a monoaxially substituted cobalt(III) phthalocyanine. Upon annealing, the axial ligand is removed with the donation of one electron to form the final CoPc monolayer. This model is supported by the fact that the N 1s peak in the XPS shifts by only 0.2 eV throughout the entire conversion process. Thus, the Pc ring is most likely in the -2 state throughout. That the final (annealed) species is unsubstituted CoPc is born out by the following: (1) the XPS spectral positions and the C/N ratio, which is identical to that of authentic CoPc, (2) the fact that the species is neutral (no alkali metal ions present), and (3) the STM images of both the individual molecules and of the overall lattice are identical to those of vapor-deposited CoPc on Au(111).

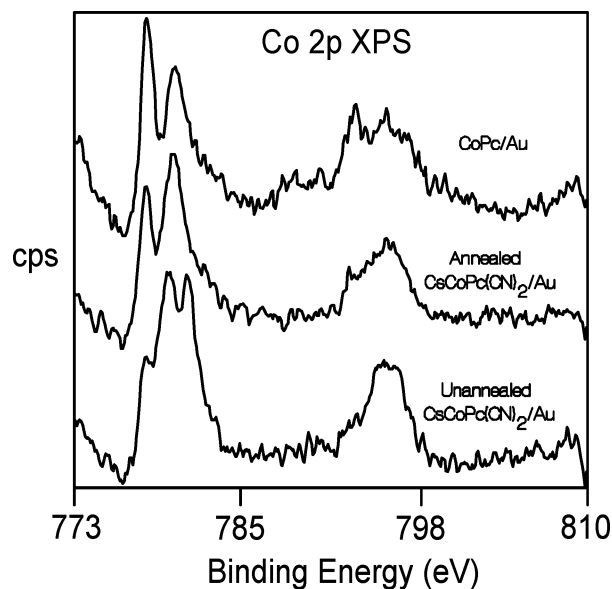


**Figure 4.** XPS of the Co 2p region of phthalocyanine complexes on Au(111).

Our proposed mechanism begins with the spontaneous oxidation of MCoPc(CN)<sub>2</sub> by gold, driven essentially by its rather large work function. To test this, we have performed XPS studies of the solution-phase adsorption on both gold and aluminum. (Al has a work function about 1 eV less than that of Au.) We find that, as expected, the initial reaction occurs rapidly with gold metal, but there is no apparent reaction with aluminum. Thus, one may envisage the selective deposition of CoPc upon gold contacts in the presence of a number of other materials (including copper, aluminum, and silicon) that have significantly smaller work functions than does gold. In fact, by tailoring the redox potential of the initial reaction and the relative solubility of the initial and final species, one could tailor the selective deposition of materials where the final product is only physisorbed to the surface. For example, a species that was reduced at about -0.4 V (sce) and became insoluble would be selectively deposited on aluminum but not on gold or silicon. In contrast, either vapor- or solution-phase deposition of the desired material would coat the entire surface.

**Acknowledgment.** We thank the National Science foundation for support in the form of grants CHE 0138409 and CHE 0234726. Acknowledgment also is made to the donors of the Petroleum Research Fund, administered by the American Chemical Society. We also thank Dr. Louis Scudiero for his assistance in acquiring the XPS data.

## References and Notes

- Hecht, S. *Angew. Chem., Int. Ed.* **2003**, *42*, 24.
- Scudiero, L.; Barlow, D. E.; Hipps, K. W. *J. Phys. Chem. B* **2000**, *104*, 11899. (b) Scudiero, L.; Barlow, Dan E.; Hipps, K. W. *J. Phys. Chem. B* **2002**, *106*, 996. (c) Hipps, K. W.; Barlow, Dan E.; Mazur, U. *J. Phys. Chem. B* **2000**, *104*, 2444. (d) Hipps, K. W.; Barlow, Dan E.; Mazur, U. *J. Phys. Chem. B* **2000**, *104*, 5993.
- Scudiero, L.; Barlow, D. E.; Mazur, U.; Hipps, K. W. *J. Am. Chem. Soc.* **2001**, *123*, 4073.
- Lei, S.; Wang, J.; Dong, Y.; Wang, C.; Wan, L.; Bai, C. *Surf. Interface Anal.* **2002**, *34*, 767. (b) Lei, S.; Wang, C.; Yin, S.; Bai, C. *J. Phys. Chem. B* **2001**, *105*, 12272. (c) Lei, S.; Wang, J.; Dong, Y.; Wang, C.; Wan, L.; Bai, C. *Surf. Interface Anal.* **2002**, *34*, 767.
- Suto, K.; Yoshimoto, S.; Itaya, K. *J. Am. Chem. Soc.* **2003**, *125*, 14976. Yoshimoto, S.; Tada, A.; Suto, K.; Itaya, K. *J. Phys. Chem. B* **2003**, *107*, 5836-5843.
- Hipps, K. W.; Scudiero, L.; Barlow, D. E.; Cooke, M. P., Jr. *J. Am. Chem. Soc.* **2002**, *124*, 2126. (b) Scudiero, L.; Hipps, K. W.; Barlow, D. E. *J. Phys. Chem. B* **2003**, *107*, 2903.

- 262 (7) Yokoyama T.; Yokoyama, S.; Kamikado, T.; Okuno, Y.; Mashiko,  
263 S. *Nature* **2001**, *413*, 619. 273
- 264 (8) Griessl, S.; Lackinger, M.; Edelwirth, M.; Hietschold, M.; Heckl,  
265 W. M. *Single Mol.* **2002**, *3*, 25. 274
- 266 (9) *An Introduction to Ultrathin Organic Films*; Ulman, A., Ed.;  
267 Academic Press: San Diego, CA, 1991. 275
- 268 (10) Mazur, U.; Hipps, K. W. *J. Phys. Chem. B* **1999**, *103*, 9721. 276
- 269 (11) Inabe, T.; Maruyama, Y. *Bull. Chem. Soc. Jpn.* **1990**, *63*, 2277. 277
- 270 (12) Leverenz, A.; Speiser, B.; Hanack, M. *J. Electroanal. Chem.* **1992**,  
271 232, 273. (b) Bchnisch, B.; Leverenz, K.; Hanack, M. *Synth. Met.* **1991**,  
272 41–43, 267. 278
- (13) Metz J.; Hanack, M. *J. Am. Chem. Soc.* **1983**, *105*, 828. (b) Orihashi,  
Y.; Nishikawa, M.; Ohno, H.; Tsuchida, E.; Matsuda, H.; Nkanishi, H.;  
Kato, M. *Bull. Chem. Soc. Jpn.* **1987**, *60*, 3731. 279
- (14) Strem Chemicals, Inc. Newburyport, MA. 280
- (15) RHK Technology, Inc. Troy, MI. 281
- (16) Yoshimoto, S.; Tada, A.; Suto, K.; Narita, R.; Itaya, K. *Langmuir*  
**2003**, *19*, 672. 282
- (17) Kim, Y. G.; Yau, S. L. Itaya, K. *J. Am. Chem. Soc.* **1996**, *118*,  
393. (b) Stuhlmann, C.; Villegas, I.; Weaver, M. J. *Chem. Phys. Lett.* **1994**,  
219, 319. 283